

# Aging dynamics across a dynamic crossover line in three dimensional short-range Ising spin glass $\text{Cu}_{0.5}\text{Co}_{0.5}\text{Cl}_2\text{-FeCl}_3$ graphite bi-intercalation compound

Itsuko S. Suzuki\* and Masatsugu Suzuki†

Department of Physics, State University of New York at Binghamton, Binghamton, New York 13902-6000

(Dated: June 14, 2018)

$\text{Cu}_{0.5}\text{Co}_{0.5}\text{Cl}_2\text{-FeCl}_3$  graphite intercalation compound is a three-dimensional short-range Ising spin glass with a spin freezing temperature  $T_c$  ( $= 3.92 \pm 0.11$  K). The stability of the spin glass phase in the presence of a magnetic field  $H$  is examined from (i) the spin freezing temperature  $T_f(\omega, H)$  at which the differential field-cooled (FC) susceptibility  $\partial M_{FC}(T, H)/\partial H$  coincides with the dispersion  $\chi'(\omega, T, H = 0)$  with the angular frequency  $\omega$ , and (ii) the time dependence of zero-field cooled (ZFC) susceptibility  $\chi_{ZFC}$  after a ZFC aging protocol with a wait time  $t_W$  ( $= 1.0 \times 10^4$ ). The relaxation rate  $S(t)$  ( $= d\chi_{ZFC}/d\ln t$ ) exhibits a local maximum at a characteristic time  $t_{cr}$ , reflecting non-equilibrium aging dynamics. The peak time  $t_{cr}(T, H)$  decreases with increasing  $H$  at the fixed temperature  $T$  ( $2.9 \text{ K} \leq T < T_c$ ). The spin freezing temperature  $T_f(\omega, H)$  provides evidence for the instability of the spin glass phase in thermal equilibrium in a finite magnetic field. Both  $t_{cr}(T, H)$  and  $T_f(\omega, H)$  exhibit certain scaling behavior predicted from the droplet picture, suggesting a dynamic crossover from SG dynamics to paramagnetic behavior in the presence of  $H$ .

PACS numbers: 75.30.Kz, 75.40.Gb, 75.60.Lr, 75.50.Lk, 75.40.Mg

## I. INTRODUCTION

It has been widely recognized that three-dimensional (3D) Ising spin glass (SG) with short range interactions undergoes a second order SG transition at least at zero magnetic field in thermal equilibrium at a finite spin freezing temperature  $T_c$ .<sup>1</sup> In spite of enormous amount of works, however, no consensus has been reached on the nature of the low temperature SG phase. Two different pictures are proposed: mean-field (MF) picture<sup>2</sup> and droplet picture.<sup>3,4</sup> In the MF picture, the low temperature SG phase exhibits a replica symmetry breaking. The SG ordered phase consists of infinite number of pure states organized in an ultrametric structure. In the droplet picture, in contrast, the SG phase is described by only two pure thermodynamic states related to each other by a global spin flip.

The stability of the Ising SG phase in an external magnetic field ( $H$ ) has been one of the central issues. In the MF picture, the phase transition can survive in the presence of low  $H$ , forming a critical line, so-called the de Almeida-Thouless (AT) line in the  $(H, T)$  phase diagram:

$$H(T) = A(1 - T/T_c)^p, \quad (1)$$

where  $A$  is a field amplitude and the exponent  $p = 3/2$ .<sup>5</sup> This line separates the paramagnetic (PM) phase from the SG phase. There is no change of symmetry at the AT transition. The correlation length and relaxation time diverge on crossing this line. In the droplet picture, no phase transition occurs in the presence of even infinitesimal  $H$  as for a ferromagnet. So there is no AT line in the  $(H, T)$  phase diagram. Any apparent transition would be an artifact related to the limited experimental time scale. Recent Monte Carlo (MC) simulations on the 3D Ising Edwards-Anderson (EA)<sup>6</sup> model with short range interactions suggest that the AT line is of dynamic origin

and vanishes in the limit of infinite times. Takayama,<sup>7</sup> and Takayama and Hukushima<sup>8</sup> have studied aging phenomena in the 3D Ising EA model under the  $H$ -shift aging protocols, using nonequilibrium Monte Carlo simulations. They have shown that the characteristic length scales associated with the  $H$ -shift aging protocols exhibit unique scaling behavior. This scaling behavior implies the instability of the SG phase in the equilibrium limit even under an infinitesimal  $H$ . Young and Katzgraber<sup>9</sup> have also studied the possibility of the AT line for the 3D EA Ising SG using MC simulations. A finite-size scaling of the correlation length shows no indication of a transition, in contrast to the zero-field case. This result also suggests that there is no AT line for the short range Ising SG. Experimentally Katori and Ito<sup>10</sup> have reported the existence of the AT line with  $p = 1.49$  in the 3D Ising SG  $\text{Fe}_{0.5}\text{Mn}_{0.5}\text{TiO}_3$ , supporting the MF picture. The critical temperature  $T_g(H)$  is determined as the one at which zero-field cooled (ZFC) susceptibility  $\chi_{ZFC}$  starts to deviate from the field-cooled (FC) susceptibility  $\chi_{FC}$ . The difference  $\Delta\chi = \chi_{FC} - \chi_{ZFC}$  is a measure for the irreversibility of the system. Mattson et al.<sup>11</sup> and Jönsson et al.<sup>12</sup> have shown from dynamic scaling analysis for the AC magnetic susceptibility of the same system that there is no SG transition in the presence of any  $H$ , supporting the droplet picture.

$\text{Cu}_{0.5}\text{Co}_{0.5}\text{Cl}_2\text{-FeCl}_3$  graphite bi-intercalation compound (GBIC) magnetically behaves like a 3D short-ranged Ising SG.<sup>13,14</sup> This compound undergoes a SG transition at  $T_c = 3.92 \pm 0.11$  K in the absence of  $H$ . We have determined the spin freezing temperature  $T_f(\omega, H)$  at which the differential FC susceptibility  $\partial M_{FC}(T, H)/\partial H$  coincides with the dispersion  $\chi'(\omega, T, H = 0)$ , where  $\omega$  ( $= 2\pi f$ ) is the angular frequency. In the present paper we report experimental result on the time dependence of  $\chi_{ZFC}$  after a ZFC aging protocol with a wait time  $t_W$  ( $= 1.0 \times 10^4$  and

$2.0 \times 10^3$  sec). We show that the relaxation rate  $S(t)$  ( $= d\chi_{ZFC}(t)/d\ln t$ ) exhibits a local maximum at a characteristic time  $t_{cr}$ , reflecting non-equilibrium aging dynamics. We find that  $t_{cr}$  decreases with increasing  $H$  at the fixed  $T$  ( $2.9 \text{ K} \leq T < T_c$ ). The experimental results of  $T_f(\omega, H)$  and  $t_{cr}(T, H)$  are discussed in terms of predictions from both the MF picture and the droplet picture (see Sec. II). We show that  $T_f(\omega, H)$  provides evidence for the instability of the SG phase in thermal equilibrium in a finite  $H$ . We also show that both  $t_{cr}(T, H)$  and  $T_f(\omega, H)$  exhibit certain scaling behavior, suggesting a dynamic crossover from SG dynamics to paramagnetic behavior in the presence of  $H$ .

## II. THEORETICAL BACKGROUND

### A. MF picture: equilibrium SG transition

In the mean-field picture, each point on the AT line in the  $H$ - $T$  phase diagram,  $T_g(H)$ , is a critical point of a continuous phase transition in the presence of  $H$  which exhibits critical divergence of the correlation length  $\xi_c(T, H)$  and the correlation time  $\tau_c(T, H)$  on approaching  $T_g(H)$  from the high-temperature side.

$$\tau_c(T, H) = \tau_0^*(\xi_c(T, H)/L_0)^z, \quad (2)$$

or

$$\tau_c(T, H) = \tau_0^*[T/T_g(H) - 1]^{-x}, \quad (3)$$

where

$$\xi_c(T, H) = L_0[T/T_g(H) - 1]^{-\nu}, \quad (4)$$

$\tau_0^*$  and  $L_0$  are microscopic units of time and length, and  $z$  and  $\nu$  are critical exponents ( $x = \nu z$ ). From the onset of the out-of-equilibrium behavior of the AC susceptibility, the freezing temperature  $T_f(\omega, H)$  can be extracted, where the probing time  $t$  is given by  $t = 2\pi/\omega$  for the AC susceptibility. Then the critical temperature  $T_g(H)$  is derived from the condition  $\tau_c(T_f, H) = t = 2\pi/\omega$ ,<sup>12</sup>

$$T_g(H) = T_f(\omega, H)/[(2\pi/\omega\tau_0^*)^{-1/x} + 1]. \quad (5)$$

If the AT line exists in the system, it is required that  $T_g(H)$  can be uniquely determined using the appropriate values of  $\tau_0^*$  and  $x$ . Note that  $\tau_0^*$  and  $x$  are assumed to be the microscopic time and the dynamic critical exponent at  $H = 0$ , respectively. The line  $T_g(H)$ , which is independent of  $\omega$ , is assumed to form an AT line of the second order in the  $H$ - $T$  plane, where  $T_g(H = 0) = T_c$ .

### B. Droplet model: scaling form for aging dynamics

The situation is rather different in the droplet model. After the SG system is cooled to  $T$  ( $< T_c$ )

through the ZFC aging protocol, the size of domain defined by  $R_T(t_a)$  grows with the age  $t_a$  from  $t_a = 0$  and reaches  $R_T(t_W)$  just before the field  $H$  is turned on at the observation time  $t = t_a - t_W = 0$  (or  $t_a = t_W$ ).<sup>8</sup> Here  $R_T(t_a)$  is expressed by

$$R_T(t_a) = L_T(t_a/\tau_0^*)^{bT/T_c}, \quad (6)$$

where  $L_T$  is a characteristic length, and  $b$  is an exponent. The aging behavior in  $\chi_{ZFC}$  is observed as a function of  $t$ . After  $t = 0$ , a probing length  $R_{tr}(t)$  corresponding to the maximum size of excitation grows with  $t$ , in a similar way as  $R_T(t_a)$ . Here  $R_{tr}(t)$  is the mean size of the subdomain in the transient regime and is expressed as<sup>8</sup>

$$R_{tr}(t) = L_T(t/\tau_0^*)^{bT/T_c}. \quad (7)$$

The quasi equilibrium relaxation occurs first through local spin arrangements in length  $R_{tr}(t) \ll R_T(t_W)$ , followed by non-equilibrium relaxation due to domain growth, when  $R_{tr}(t) \approx R_T(t_W)$ , so that a crossover between the short-time quasi-equilibrium relaxation and the non-equilibrium relaxation at longer observation times is expected to occur near  $t \approx t_W$ . In the time range  $0 < t < t_{cr}$ , which we call the transient regime of  $H$ -shift processes, SG domains in local equilibrium with respect to  $H > 0$  grow within the SG domains which were in local equilibrium with respect to  $H = 0$  at  $t_a = t_W$ .

Here we introduce two characteristic lengths  $R_W$  and  $R_{cr}$  defined by

$$R_W = R_T(t_a = t_W) = L_T(t_W/\tau_0^*)^{bT/T_c}, \quad (8a)$$

$$R_{cr} = R_{tr}(t = t_{cr}) = L_T(t_{cr}/\tau_0^*)^{bT/T_c}, \quad (8b)$$

and the magnetic field crossover length  $R_H$  defined by<sup>12</sup>

$$R_H \approx l_H[(1 - T/T_c)^{a_{eff}} H^{-1}]^\delta, \quad (8c)$$

where  $l_H$  is a constant associated with a characteristic length,  $\delta = (d/2 - \theta)^{-1}$  and  $a_{eff} = \theta\nu - \beta/2$ . The definition of  $d$ ,  $\theta$ ,  $\beta$ , and  $\nu$  is given in the previous paper.<sup>13</sup> According to Takayama and Hukushima,<sup>8</sup> it is predicted that  $Y$  ( $= R_{cr}/R_H$ ) is described by a scaling function of  $X$  ( $= R_W/R_H$ ):

$$Y = R_{cr}/R_H = f(R_W/R_H) = f(X). \quad (9)$$

The  $H$ -shift aging process is nothing but a dynamic crossover from the SG phase in  $H = 0$  to the paramagnetic state in  $H > 0$  in the equilibrium limit. In the limit of large  $R_W/R_H$ ,  $R_{cr}/R_H$  becomes constant.

For the AC magnetic susceptibility measurement with the angular frequency  $\omega$ , the size  $R_{tr}(t = 2\pi/\omega)$  is the mean size of droplets that can respond to the AC field of frequency  $\omega$ . Then the onset of the SG out-of-equilibrium dynamics,  $T_f(t, H)$ , can be related to  $R_H$  by the condition,<sup>12</sup>

$$R_H = R_{tr}(t = 2\pi/\omega), \quad (10a)$$

or

$$(1 - T_f(\omega, H)/T_c)^{a_{eff}}/H = (L_T/l_H)^{1/\delta} [(2\pi/\omega\tau_0^*)^{T_f(t, H)/T_c}]^{b/\delta}. \quad (10b)$$

### III. EXPERIMENTAL PROCEDURE

The detail of sample characterization and sample preparation of  $\text{Cu}_{0.5}\text{Co}_{0.5}\text{Cl}_2\text{-FeCl}_3$  GBIC was provided in our previous papers.<sup>13,14</sup> The DC magnetization was measured using a SQUID magnetometer (Quantum Design, MPMS XL-5) with an ultra low field capability option. The remnant magnetic field was reduced to zero field (exactly less than 3 mOe) at 298 K. The time ( $t$ ) dependence of the zero-field cooled (ZFC) magnetization ( $M_{ZFC}$ ) was measured at fixed points in the ( $H, T$ ) plane. The following ZFC aging protocol was made before the measurement. First the sample was annealed at 50 K for  $1.2 \times 10^3$  sec in the absence of  $H$ . Then the system was quenched from 50 K to  $T (< T_c)$ . It was kept at  $T$  for a wait time  $t_W$  ( $= 2.0 \times 10^3$  sec and  $1.0 \times 10^4$  sec). After the wait time, an external magnetic field  $H$  is applied along any direction perpendicular to the  $c$ -axis at  $t = 0$  (or  $t_a = t_W$ ), where  $t_a$  is an age and  $t$  is an observation time ( $t_a = t + t_W$ ). The measurements of  $\chi_{ZFC}$  vs  $t$  were carried out at the fixed  $T$  ( $2.9 \leq T < T_c$ ) when  $H$  is varied as a parameter:  $1 \leq H \leq 400$  Oe.

Under the above conditions,  $\chi_{ZFC}(t)$  ( $= M_{ZFC}(t)/H$ ) was measured as a function of  $t$ . The relaxation rate defined by  $S(t)$  ( $= d\chi_{ZFC}(t)/d\ln t$ ) exhibits a peak at a characteristic time  $t_{cr}$ .<sup>15</sup> Theoretically<sup>16,17</sup> and experimentally<sup>18,19,20</sup> it has been accepted that the time variation of  $\chi_{ZFC}(t)$  may be described by a stretched exponential relaxation form:

$$\chi_{ZFC}(t) = \chi_0 - B_0 t^{-m} \exp[-(t/\tau)^{1-n}], \quad (11)$$

where the exponent  $m$  may be positive and is very close to zero,  $n$  is between 0 and 1,  $\tau$  is a characteristic relaxation time,  $\chi_0$ ,  $m$ , and  $B_0$  are constants, and  $n$  is a stretched exponential exponent. The least-squares fit of the data of  $\chi_{ZFC}$  vs  $t$  to Eq.(11) with  $m = 0$  yields the parameters  $n$ ,  $\tau$ , and  $B_0$  as a function of  $H$  and  $T$  in the  $H$ - $T$  plane.

### IV. RESULT

#### A. Line $T_{g_0}(H)$ from the measurement of $d\Delta\chi/dT$ vs $T$

In our previous paper<sup>13</sup> we have discussed the  $H$  dependence of the spin freezing temperature in detail. The result is summarized as follows. Figure 1(a) shows the  $T$  dependence of the difference between  $\chi_{FC}$  and  $\chi_{ZFC}$  ( $\Delta\chi = \chi_{FC} - \chi_{ZFC}$ ) at various  $H$  in the vicinity of  $T_c$ . The transition temperature is defined as a temperature at which  $\Delta\chi = 0$ . Since it is difficult to determine exactly the transition temperature from Fig. 1(a), we redefine the line  $T_{g_0}(H)$  as one at which  $d\Delta\chi/dT$  vs  $T$  shows a local minimum for each  $H$  (see Fig. 1(b)). In Fig. 2 we show the  $H$  dependence of  $T_{g_0}(H)$  thus obtained. The least squares fit of the data of  $H$  vs  $T$  (or  $H$  vs  $T_{g_0}(H)$ ) in Fig. 2 to Eq.(1) yields the parameters  $p$  and  $A$ , where

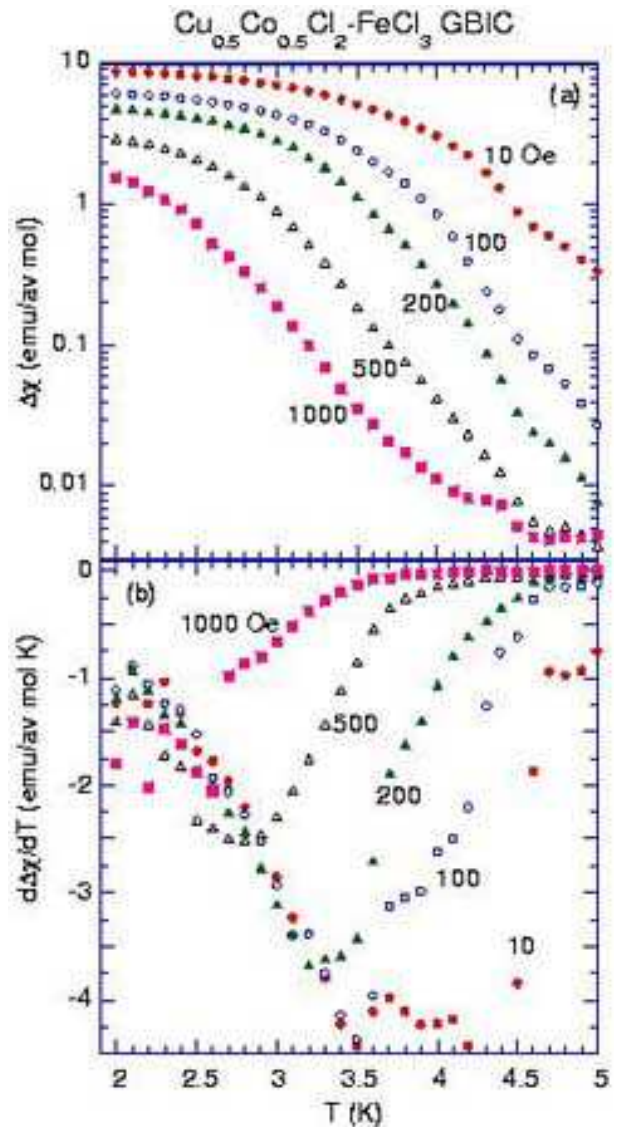


FIG. 1: (Color online)  $T$  dependence of (a)  $\Delta\chi = \chi_{FC} - \chi_{ZFC}$  and (b)  $d\Delta\chi/dT$  at various  $H$  for  $\text{Cu}_{0.5}\text{Co}_{0.5}\text{Cl}_2\text{-FeCl}_3$  GBIC.

$T_c$  is fixed as  $T_c = 3.92 \pm 0.11$  K. The exponent  $p$  is equal to  $1.52 \pm 0.10$ , which is close to the AT exponent ( $p = 3/2$ ). The value of  $A$  is  $A_{exp} = 3.38 \pm 0.67$  kOe. For convenience, hereafter this critical line is denoted as the line  $T_{g_0}(H)$  ( $d\Delta\chi/dT$  vs  $T$ ). In the classical  $q$  vector SG model, the value of  $A$  is predicted as<sup>18,21</sup>

$$A_{theory} = [8/(q+1)(q+2)]^{1/2} (k_B T_c / g \mu_B S), \quad (12)$$

where  $S$  is the spin,  $g$  is the Landé  $g$ -factor, and  $q$  is the number of spin degrees of freedom ( $q = 1$  for Ising SG and  $q = 3$  for Heisenberg SG). Here we assume  $g = 2$ . The value of  $S$  is estimated as  $S = 1.56$  for our system with the stoichiometry  $\text{C}_{5.26}(\text{Cu}_{0.5}\text{Co}_{0.5}\text{Cl}_2)_{0.47}(\text{FeCl}_3)_{0.53}$ ,<sup>13</sup> where  $S = 1/2$  for  $\text{Co}^{2+}$  and  $\text{Cu}^{2+}$  and  $S = 5/2$  for  $\text{Fe}^{3+}$ . Then the value of  $A_{theory}$  is estimated as 21.6 kOe for  $q = 1$  (Ising symmetry), leading to  $A_{exp}/A_{theory} = 0.16$ .

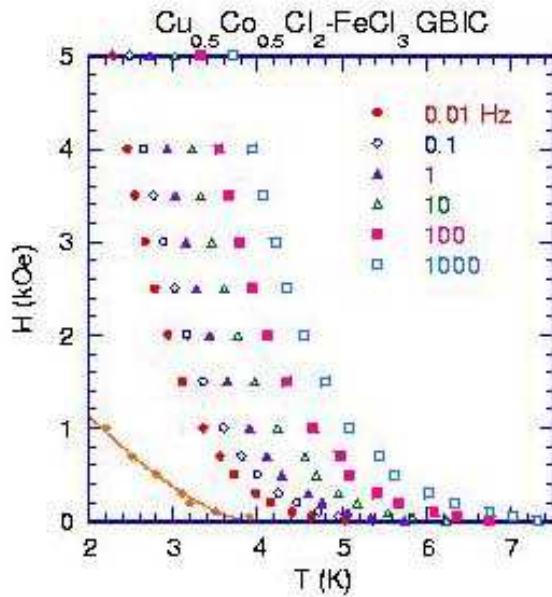


FIG. 2: (Color online)  $H$ - $T$  phase diagram. (i) The local minimum temperature of  $d\Delta\chi/dT$  vs  $T$  at  $H$  ( $\blacklozenge$ ) [denoted as the line  $T_{g0}(H)$  ( $d\Delta\chi/dT$  vs  $T$ )]. A solid line is a least-squares fitting curve which is expressed by Eq.(1) with  $T_c$ ,  $p$  and  $A$  given in the text. (ii)  $T_f(\omega, H)$  vs  $H$  between  $f = 0.01$  Hz and 1 kHz.  $T_f(\omega, H)$  is defined as a temperature at which  $\chi_{FC}(T, H)$  crosses  $\chi'(\omega, T, H = 0)$  at each  $\omega$ .

These results are similar to those reported by Katori and Ito<sup>10</sup> for  $\text{Fe}_{0.5}\text{Mn}_{0.5}\text{TiO}_3$ :  $p = 1.49$  and  $A_{exp}/A_{theory} = 0.52$  ( $A_{exp} = 42.6$  kOe,  $A_{theory} = 82.1$  kOe). Although such result apparently supports the AT theory, it does not provide any evidence for an equilibrium SG transition in the presence of  $H$ .

### B. Line $T_f(\omega, H)$ where $\partial M_{FC}(T, H)/\partial H = \chi'(\omega, T, H = 0)$

In our previous paper<sup>13</sup> we have discussed the spin freezing temperature  $T_f(\omega, H)$  of  $\text{Cu}_{0.5}\text{Co}_{0.5}\text{Cl}_2\text{-FeCl}_3$ , at which  $\partial M_{FC}(T, H)/\partial H$  crosses the dispersion  $\chi'(\omega, T, H = 0)$  at each  $f$ . Such definition of  $T_f(\omega, H)$  has been also used by Mattsson et al.<sup>11</sup> and Jönsson et al.<sup>12</sup> for  $T_f(\omega, H)$  in  $\text{Fe}_{0.5}\text{Mn}_{0.5}\text{TiO}_3$ . In Fig. 2, we show the plot of  $T_f(\omega, H)$  as a function of  $H$  where  $f$  ( $0.01 \leq f \leq 1000$  Hz) is varied as a parameter. The line  $T_f(\omega, H)$  is strongly dependent on  $f$ . If  $T_f(\omega, H)$  in the limit of  $f = 0$  coincides with the line  $T_{g0}(H)$  ( $d\Delta\chi/dT$  vs  $T$ ) as shown in Fig. 2, then this line would be an equilibrium AT line.

It has been reported that the SG phase transition occurs only at zero field in  $\text{Fe}_{0.5}\text{Mn}_{0.5}\text{TiO}_3$ .<sup>11,12</sup> The disappearance of the AT line at finite fields is consistent with the prediction derived from the droplet picture. By using the same method (see Sec. II), here we examine whether

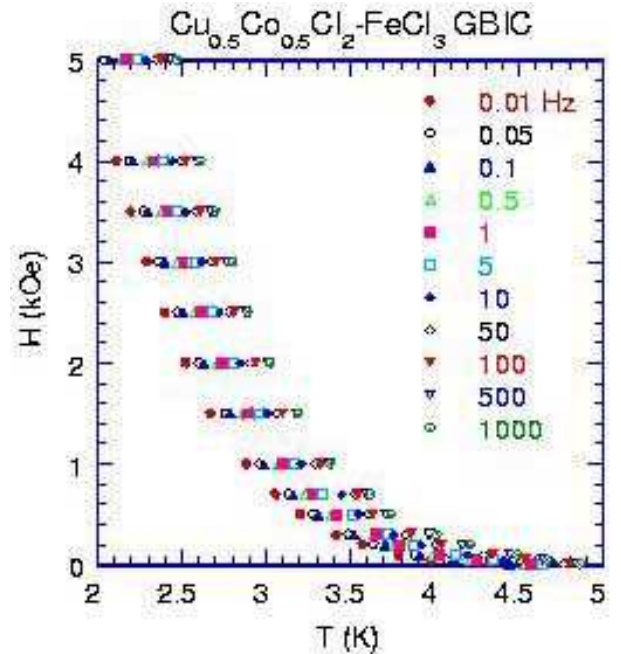


FIG. 3: (Color online) Plot of  $T_g(H)$  ( $= T_f(\omega, H)/[1 + (2\pi/\omega\tau_0^*)^{-1/x}]$ ) vs  $H$  with  $x = 10.3$  and  $\tau_0^* = 5.27 \times 10^{-6}$  sec, where  $\omega$  ( $= 2\pi f$ ) is the angular frequency.

the system exhibits the critical slowing down in the presence of  $H$ . If the SG transition occurs at  $T_g(H)$  in thermal equilibrium as is predicted from the MF picture, it is required that the critical temperature  $T_g(H)$  evaluated from Eq.(5) should fall on a unique curve  $T = T_g(H)$ , which is independent of  $\omega$ .

We calculate the line  $T_g(H)$  using Eq.(5) with the data of  $T_f(\omega, H)$  for each  $\omega$ . Here we use  $\tau_0^* = 5.27 \times 10^{-6}$  sec,  $T_c = 3.92$  K, and  $x = z\nu = 10.3$ , which are obtained from the analysis of the absorption  $\chi''(\omega, T, H = 0)$  in the previous paper.<sup>13</sup> Figure 3 shows the line  $T_g(H)$  thus obtained. We find that the line  $T_g(H)$  is still strongly dependent on  $\omega$ , although the line  $T_g(H)$  tends to approach the line  $T_{g0}(H)$  ( $d\Delta\chi/dT$ ). We note that the line  $T_g(H)$  is still dependent of  $\omega$  even if  $x$  is equal to 20, which is unphysically large. This result suggests that no equilibrium SG phase transition occurs in the presence of  $H$ , which is inconsistent with the prediction from the MF picture.

Now we examine the validity of the droplet picture. As is described in Sec. II, the onset of the SG out-of-equilibrium dynamics,  $T_f(t, H)$ , is related to  $R_H$  by Eq.(10b) with  $X_1 = (t/\tau_0^*)^{T_f(t, H)/T_c}$  and  $t = 2\pi/\omega$ .<sup>12</sup> When  $Y_1$  is defined as  $Y_1 = (1 - T_f(t, H)/T_c)^{a_{eff}}/H$ , Eq.(10b) is rewritten as

$$Y_1 \approx \zeta^{1/\delta} X_1^{b/\delta}, \quad (13)$$

with  $\zeta = L_T/l_H$ . Figure 4 shows the plot of  $\ln(Y_1)$  as a function of  $\ln(X_1)$  with the best choice of  $a_{eff} = 0.55 \pm 0.05$ , where  $\tau_0^* = 5.27 \times 10^{-6}$  sec. When only the data with

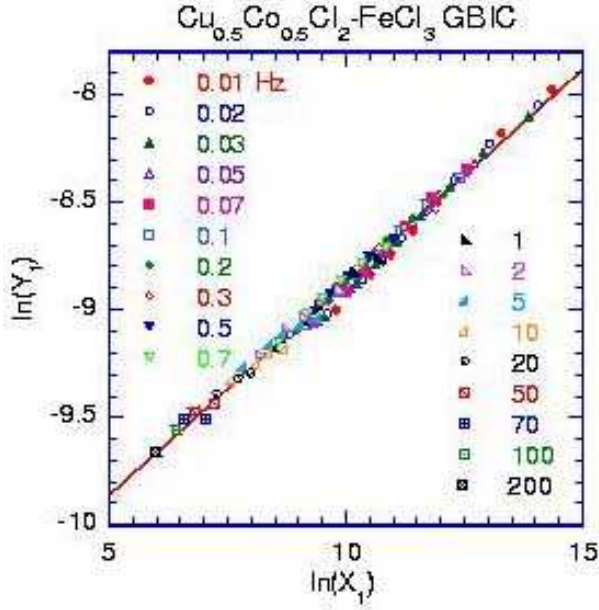


FIG. 4: (Color online) Scaling plot of  $\ln(Y_1)$  vs  $\ln(X_1)$  for the data with  $T_f(\omega, H)/T_c \leq 0.9$ , where  $Y_1 = (1 - T_f(\omega, H)/T_c)^{a_{eff}}/H$  and  $X_1 = (2\pi/\omega\tau_0^*)^{T_f(t, H)/T_c}$ . The best result for the scaling plot is obtained when  $a_{eff} = 0.55$ , where  $T_c$  ( $= 3.92$  K) and  $\tau_0^*$  ( $= 5.27 \times 10^{-6}$  sec) are fixed. The least-squares fitting curve ( $Y_1 \approx \zeta^{1/\delta} X_1^{b/\delta}$ ) is denoted by a straight line with a slope of  $b/\delta = 0.194$  and  $\zeta = 1.5 \times 10^{-4}$  ( $\delta = 0.81$ ).

$T_f(t, H)/T_c < 0.9$  are used, almost all the data fall well on an unique straight line with the slope  $b/\delta = 0.198 \pm 0.002$  and  $\ln(\zeta^{1/\delta}) = -10.85 \pm 0.02$ . Using the value of  $b = 0.16$  for  $\chi''(\omega, T = 3.75$  K,  $t$ ) with  $f = 0.05$  Hz,<sup>13</sup>  $\delta$  can be estimated as  $\delta = 0.81$ . This value of  $\delta$  is slightly deviated from the calculated value of  $\delta$  using the relation  $\delta = (d/2 - \theta)^{-1} = 0.73$  with  $d = 3$  and  $\theta = 0.13$ . Our value of  $a_{eff}$  is much larger than the value predicted from the relation ( $a_{eff} = \theta\nu - \beta/2 \approx 0$ ), where  $\beta = 0.36 \pm 0.03$ ,  $\nu = 1.4 \pm 0.2$ , and  $\theta = 0.13 \pm 0.02$  which are obtained in the previous paper.<sup>13</sup> Using  $\delta = 0.81$ , the value of  $\zeta$  is calculated as  $(1.5 \pm 0.1) \times 10^{-4}$ . This value will be used in Sec. V. It is interesting to compare our result with that reported by Jönsson et al. for  $\text{Fe}_{0.5}\text{Mn}_{0.5}\text{TiO}_3$ .<sup>12</sup> They have reported the values of  $a_{eff} = 0.45$  and  $b/\delta = 0.17$  for the high-temperature (HT) data with  $T_f(\omega, H)/T_c \leq 0.95$  and  $H \leq 5$  kOe, and  $a_{eff} = 0.25$ ,  $b/\delta = 0.143$  for the low-temperature (LT) data, where  $\theta = 0.2$  and  $\delta = 0.77$ . Our result ( $a_{eff} = 0.55$  and  $b/\delta = 0.198$ ) is close that obtained from the HT data.

### C. Stretched exponential relaxation form $\chi_{ZFC}(t)$ at $H = 1$ Oe

We have measured the  $t$  dependence of  $\chi_{ZFC}(t)$  after the ZFC aging protocol described in Sec. III. Figures 5(a) and (b) show the  $t$  dependence of  $\chi_{ZFC}(t)$

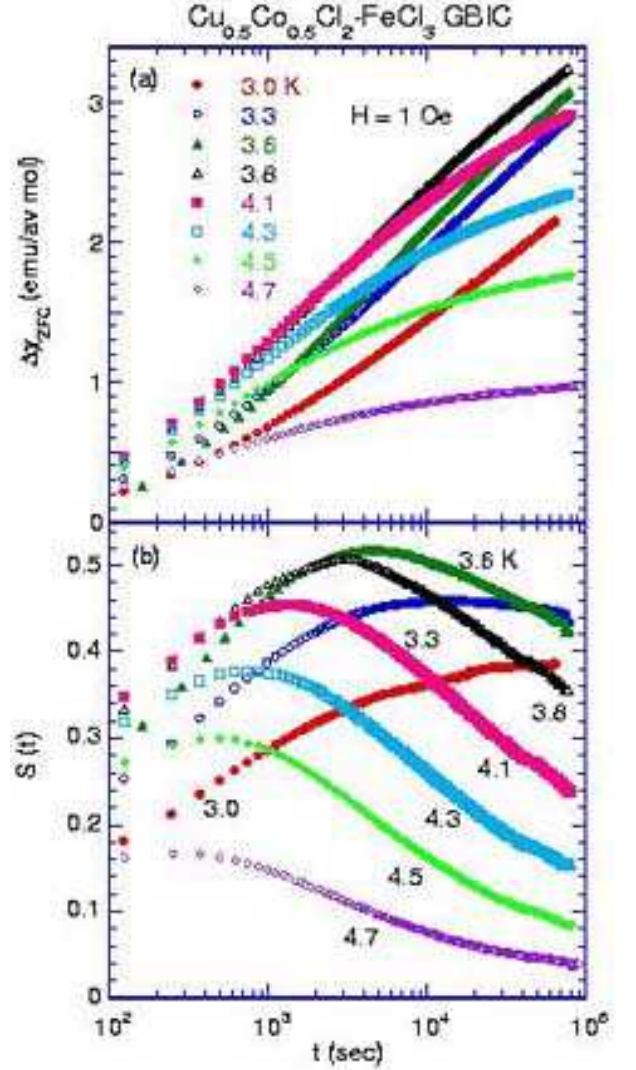


FIG. 5: (Color online)  $t$  dependence of (a)  $\Delta\chi_{ZFC}(t)$  [ $= \chi_{ZFC}(t) - \chi_{ZFC}(t = 0)$ ] and (b) the relaxation rate  $S(t)$  ( $= d\chi_{ZFC}(t)/d\ln t$ ) at various  $T$  ( $3.0 \leq T \leq 4.7$  K).  $t_W = 2.0 \times 10^3$  sec.  $H = 1$  Oe.

and the relaxation rate  $S(t)$  at various  $T$ , respectively, where  $t_W = 2.0 \times 10^3$  sec and  $H = 1$  Oe. The relaxation rate  $S(t)$  exhibits a peak at  $t = t_{cr}$ , which shifts to the short- $t$  side with increasing  $T$ . The ZFC susceptibility  $\chi_{ZFC}(t)$  is well described by Eq.(11) with  $m = 0$  for  $1.0 \times 10^2 < t < 6.0 \times 10^4$  sec. The least-squares fit of the data of  $\chi_{ZFC}$  vs  $t$  yields the parameters  $n$  and  $\tau$  for each  $T$ . In Fig. 6(a), we show the  $T$  dependence of  $t_{cr}$  and  $\tau$ . Both  $t_{cr}$  and  $\tau$  increase with decreasing  $T$ :  $\tau = 3.4 \times 10^4$  sec at  $T = 3$  K. Note that  $\tau$  is larger than  $t_{cr}$  below  $T_c$ . In the inset of Fig. 6(a) we show the plot of  $1/t_{cr}$  and  $1/\tau$  as a function of  $1/T$ . The least-squares fit of the data of  $1/\tau$  vs  $1/T$  for  $T < T_c$  to the form<sup>18</sup>

$$1/\tau = c_1 \exp(-c_2 T_c/T), \quad (14)$$

yields the parameters  $c_1 = 19.7 \pm 11.5$  sec<sup>-1</sup> and  $c_2 = 10.82 \pm 0.56$ . For the data of  $1/t_{cr}$  vs  $1/T$ , similarly we

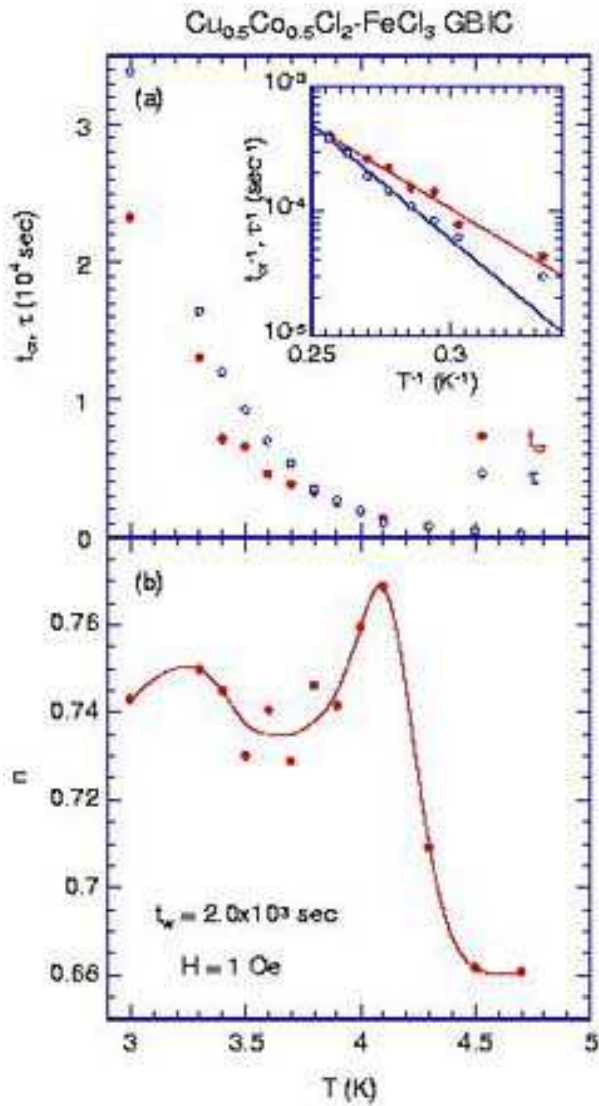


FIG. 6: (Color online) (a)  $T$  dependence of  $t_{cr}$  and  $\tau$ .  $t_{cr}$  is a characteristic time at which  $S(t)$  exhibits a peak and  $\tau$  is the relaxation time for the stretched exponential relaxation.  $H = 1$  Oe.  $t_w = 2.0 \times 10^3$  sec. The inset shows the plots of  $1/t_{cr}$  vs  $1/T$  and  $1/\tau$  vs  $1/T$  for  $T < T_c$ . The solid lines are least-squares fits to Eq.(14) for both  $1/t_{cr}$  vs  $1/T$  and  $1/\tau$  vs  $1/T$ . The fitting parameters are given in the text. (b)  $T$  dependence of the stretched exponential exponent  $n$ . The solid line is a guide to the eyes.

obtain  $c_1 = 1.01 \pm 0.48 \text{ sec}^{-1}$  and  $c_2 = 7.81 \pm 0.46$ . Note that our value of  $c_2$  is much larger than those derived by Hoogerbeets et al.<sup>18</sup> ( $c_2 = 2.5$ ) from their analysis of thermoremanent magnetization (TRM) relaxation measurements on four canonical SG systems: Ag: Mn (2.6 at. %), Ag: Mn (4.1 at. %), Ag: [Mn (2.6 at. %) + Sb (0.46 at. %)], and Cu: Mn (4.0 at. %). Note that in their work the stretched exponential is taken as representative of the short time ( $t < t_w$ ) relaxation. In Fig. 6(b) we show the  $T$  dependence of  $n$ . The exponent  $n$  exhibits a local maximum around  $T = 3.3$  K ( $T/T_c = 0.84$ ), a local

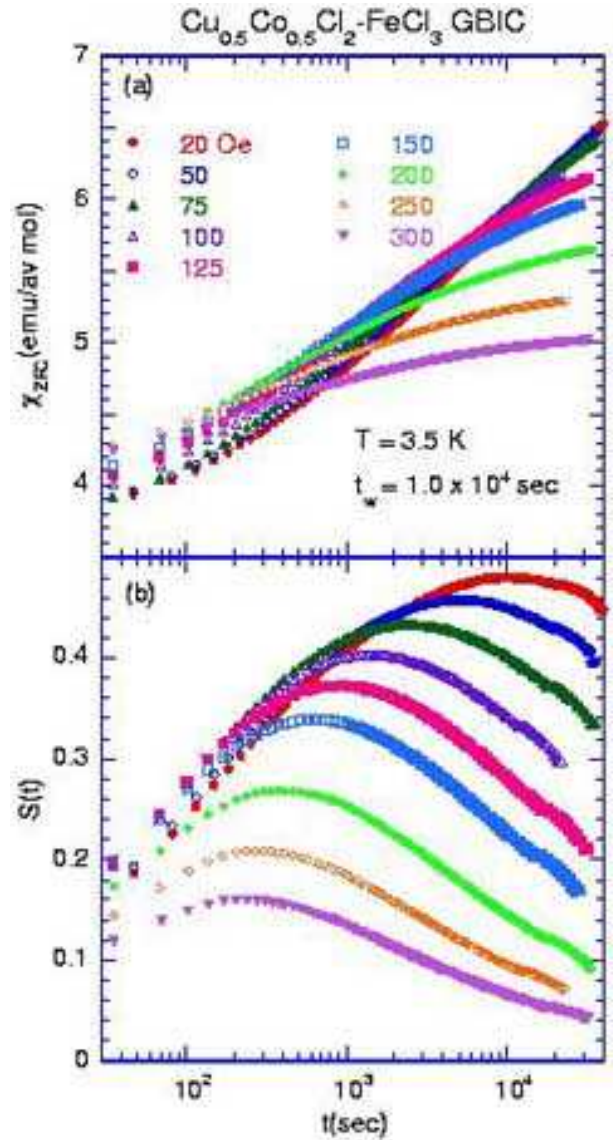


FIG. 7: (Color online)  $t$  dependence of (a)  $\chi_{ZFC}(t)$  and (b)  $S(t)$  at various  $H$  ( $20 \leq H \leq 300$  Oe).  $t_w = 1.0 \times 10^4$  sec.  $T = 3.50$  K.

minimum around 3.5 - 3.7 K ( $T/T_c = 0.89 - 0.94$ ), and a sharp peak just above  $T_c$ . It drastically decreases with further increasing  $T$  above  $T_c$ . The overall variation of  $n$  below  $T_c$  is similar to that reported by Bontemps<sup>22</sup> and Bontemps and Orbach<sup>23</sup> for  $\text{Eu}_{0.4}\text{Sr}_{0.6}\text{S}$  ( $T_c = 1.50$  K):  $n$  has a local maximum at  $T/T_c = 0.87$ , a local minimum at  $T/T_c = 0.91$ , and a local maximum at  $T = T_c$ . In summary, the transition between the SG and PM phases at  $H = 1$  Oe is characterized by the peak of  $n$  and the drastic increase of  $t_{cr}$  (or  $\tau$ ) with decreasing  $T$  around  $T_c$ .

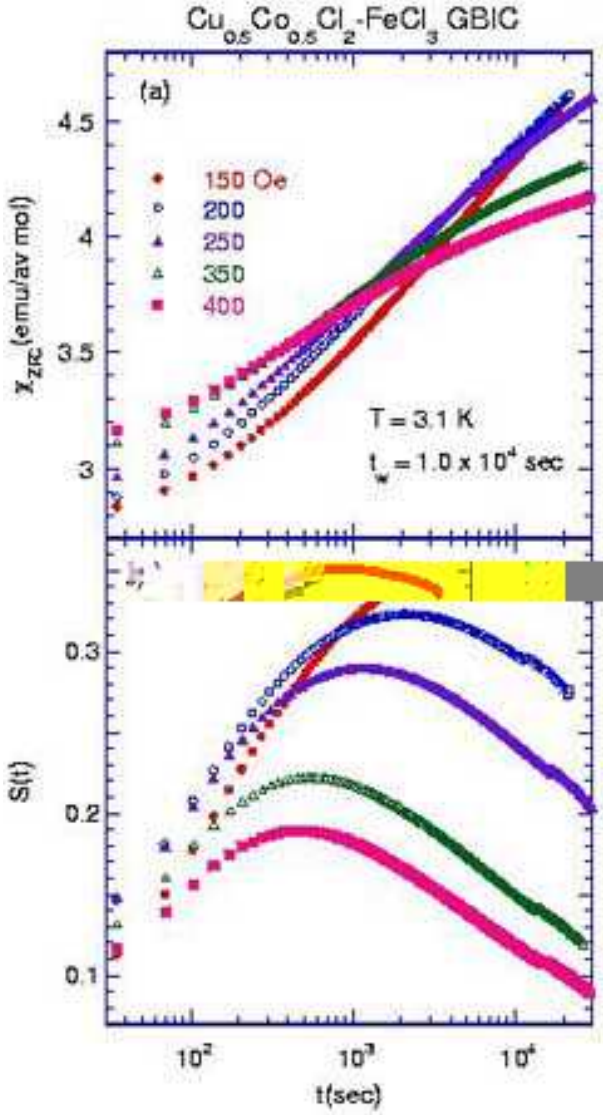


FIG. 8: (Color online)  $t$  dependence of (a)  $\chi_{ZFC}(t)$  and (b)  $S(t)$  at various  $H$  ( $150 \leq H \leq 400$  Oe).  $t_W = 1.0 \times 10^4$  sec.  $T = 3.10$  K.

#### D. $H$ and $T$ dependence of $t_{cr}$ and $\tau$

We have also measured the  $t$  dependence of  $\chi_{ZFC}(t)$  after the same ZFC aging protocol described in Sec. III, where  $t_W = 1.0 \times 10^4$  sec,  $T = 2.9, 3.0, 3.1, 3.3, 3.5, 3.65,$  and  $3.75$  K and  $H = 20, 50, 100, 150, 200, 300,$  and  $400$  Oe. Figures 7(a) and (b) show the  $t$  dependence of  $\chi_{ZFC}(t)$  and  $S(t)$  at  $T = 3.5$  K, respectively. Figures 8(a) and (b) show the  $t$  dependence of  $\chi_{ZFC}(t)$  and  $S(t)$  at  $T = 3.1$  K, respectively. Here  $H$  is chosen such that the point at  $(T, H)$  crosses the line  $T_{g0}(H)$  ( $d\Delta\chi/dT$  vs  $T$ ) in the  $H$ - $T$  plane. The relaxation  $S(t)$  has a peak at  $t = t_{cr}$ , which shifts to the low- $t$  side with increasing  $H$ . The peak height of  $S(t)$  at  $t = t_{cr}$  drastically decreases with increasing  $H$ . The least-squares fit of the data of  $\chi_{ZFC}(t)$  vs  $t$  for  $1.0 \times 10^2$  sec  $< t < t_W$  to Eq.(11) with

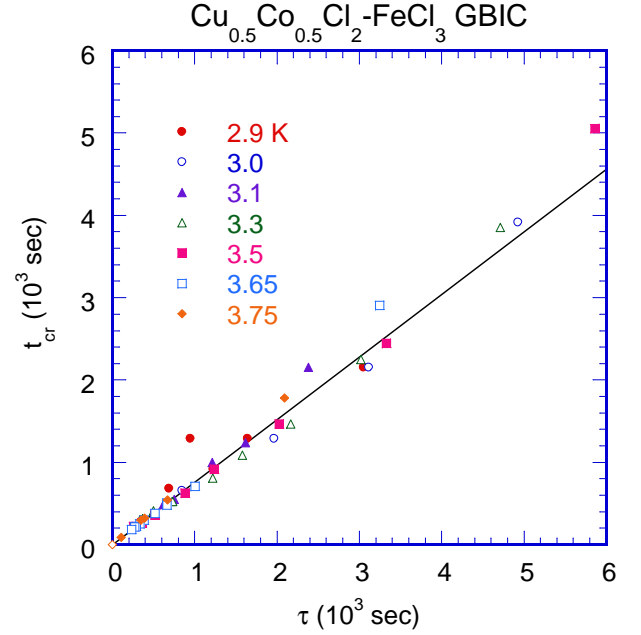


FIG. 9: (Color online) Plot of  $t_{cr}$  vs  $\tau$  for various  $H$  between 50 and 400 Oe at each  $T$ . A solid line is a least-squares fitting curve denoted by  $x_{cr} = t_{cr}/\tau = 0.80$ .  $t_W = 1.0 \times 10^4$  sec.

$m = 0$  yields the exponent  $n$  and  $\tau$  at each  $H$  and  $T$ , where  $\tau$  is the relaxation time of the stretched exponential relaxation. Note that the data ( $\chi_{ZFC}$  vs  $t$ ) are not fitted well with Eq.(11) with  $m \neq 0$ : the value of  $n$  is dependent on the small change in  $m$ .

The values of  $\tau$  and  $t_{cr}$  have been determined from the  $t$  dependence of  $\chi_{ZFC}(t)$  and  $S(t)$  at fixed  $H$  and  $T$ . In Fig. 9 we make a plot of  $t_{cr}$  vs  $\tau$  at each  $T$  ( $2.9 \leq T \leq 3.75$  K) for measured values of  $H$ . We find that  $t_{cr}$  is proportional to  $\tau$  in the range  $0 \leq \tau \leq 6.0 \times 10^3$  sec:  $x_{cr} = t_{cr}/\tau = 0.80 \pm 0.01$ . This ratio is different from the ratio ( $x_{cr} = 1$ ) predicted from Eq.(11) with  $m = 0$ , which is independent of  $n$ . A slight deviation from this linear relation is observed for  $\tau > 6.0 \times 10^3$  corresponding to the case of low  $H$  ( $H < 50$  Oe), partly because of the larger uncertainty in  $\tau$ . Since the  $H$  and  $T$  dependence of  $t_{cr}$  is essentially the same as that of  $\tau$ , hereafter we discuss only the  $H$  and  $T$  dependence of  $t_{cr}$ . Figure 10(a) shows the  $H$  dependence of  $t_{cr}$  at fixed  $T$  ( $2.9 \leq T \leq 3.75$  K) below  $T_c$ . At higher  $T$ , the decrease of  $t_{cr}$  with  $H$  occurs at lower  $H$ . Figure 10(b) shows the  $T$  dependence of  $t_{cr}$  at fixed  $H$  below  $T_c$ .

## V. DISCUSSION

We examine the validity of the scaling relation given by Eq.(9) using the data of  $t_{cr}(T, H)$  with  $t_W = 1.0 \times 10^4$  sec in Figs. 10(a) and (b). Note that  $t_{cr}(T, H)$  is the peak time of  $S(t)$  vs  $t$  for  $2.9 \leq T \leq 3.75$  K and  $5 \leq H \leq 500$  Oe. We define the following two parameters

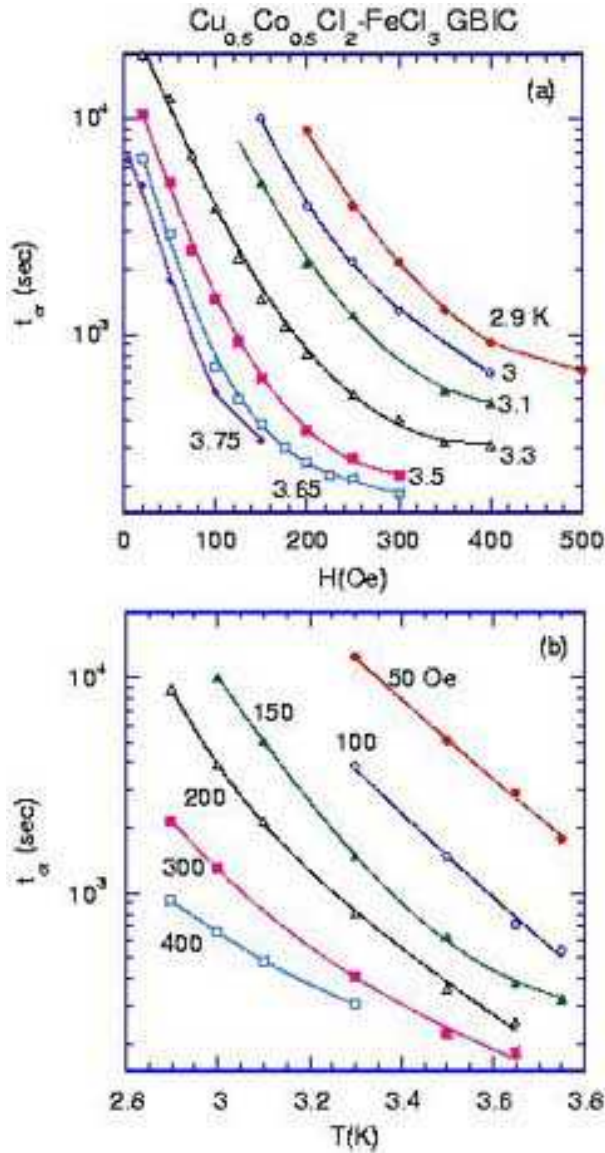


FIG. 10: (Color online) (a)  $t_{cr}$  vs  $H$  at various  $T$  and (b)  $t_{cr}$  vs  $T$  at various  $H$ . The solid lines are guides to the eyes.

$X$  and  $Y$  given by

$$X = \zeta [H^{\delta/b} (t_W / \tau_0^*)^{T/T_c} (1 - T/T_c)^{-(\delta/b)a_{eff}}]^b, \quad (15a)$$

and

$$Y = \zeta [H^{\delta/b} (t_{cr}(T, H) / \tau_0^*)^{T/T_c} (1 - T/T_c)^{-(\delta/b)a_{eff}}]^b, \quad (15b)$$

respectively. In Figs. 11(a) and (b) we show a scaling plot of  $Y$  vs  $X$  with  $\tau_0^* = 5.27 \times 10^{-6}$  sec and  $T_c = 3.92$  K. If we use the parameters  $\delta/b (= 5.05)$ ,  $a_{eff} (= 0.55)$ , and  $\zeta (= 1.5 \times 10^{-4})$ , which are determined independently from Fig. 4, we find that almost all the points  $(X, Y)$  fall well on a single curve. Here we use the value of  $b (= 0.16)$ .<sup>13</sup> In fact, the scaling form of Figs. 11(a) and (b) is not so sensitive to the choice of  $b$  for  $0.14 \leq b \leq 0.18$ . Similar scaling curve has been reported by Jönsson et al.<sup>24,25</sup>

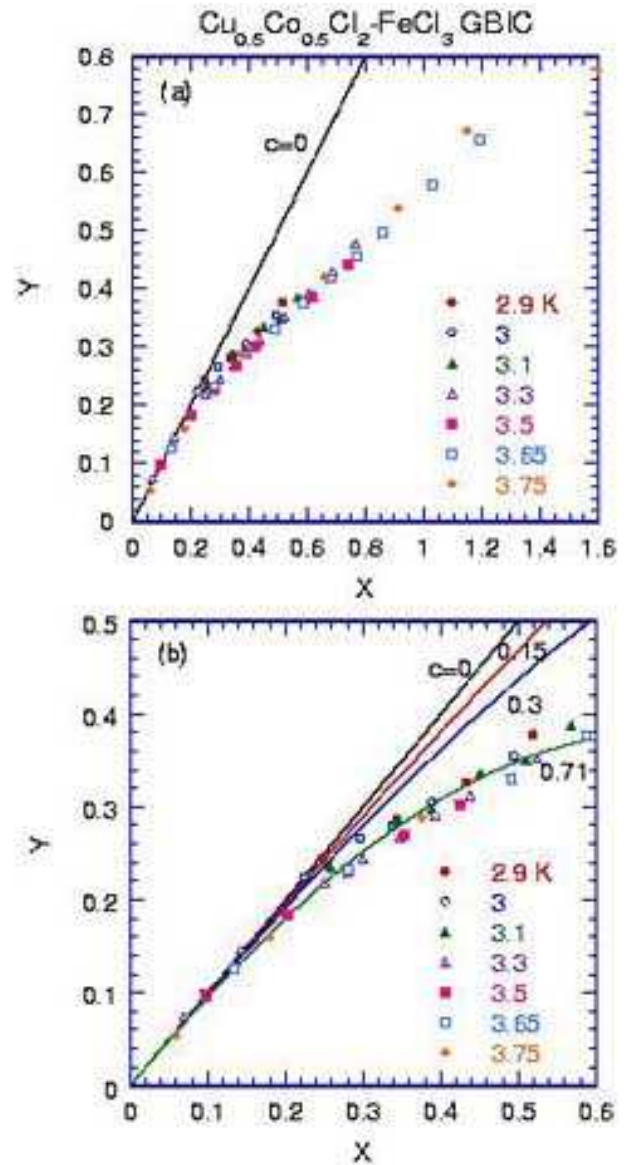


FIG. 11: (Color online) (a) Scaling plot of  $Y$  vs  $X$ .  $X$  and  $Y$  are defined by Eqs.(15a) and (15b), respectively, where  $\delta/b = 5.15$ ,  $b = 0.16$ ,  $a_{eff} = 0.55$ ,  $\zeta = 1.5 \times 10^{-4}$ ,  $T_c = 3.92$  K, and  $\tau_0^* = 5.27 \times 10^{-6}$  sec.  $t_{cr}$  is a time of the peak for  $S(t)$  vs  $t$  with  $t_W = 1.0 \times 10^4$  sec for  $2.9 \leq T \leq 3.75$  K and  $5 \leq H \leq 500$  Oe. (b) The same scaling plot of  $Y$  vs  $X$  for  $0 \leq X \leq 0.6$ . The solid lines are denoted by Eq.(16) with  $c = 0, 0.15, 0.3$ , and  $0.71$  where  $\delta = 0.81$ . Note that the solid line with  $c = 0.71$  also coincides with that derived from the least-squares fit of the data to Eq.(16) with  $c = 0.71 \pm 0.06$  and  $\delta = 0.81 \pm 0.07$ .

from the aging behavior of  $\chi_{ZFC}(t)$  for Ag 11 at. % Mn under the  $T$ -shift protocol.

Our curve is well described by a straight line given by  $Y = X$  for  $X \leq 0.1$ . It deviates from the straight line with increasing  $X$  and tends to saturate around  $X \approx 1.6$ . There is a gradual crossover between accumulative and chaos around  $X = 0.1$ . Our curve is similar to a scaling



curve of  $Y$  vs  $X$  which is predicted by Takayama and Hukushima<sup>8</sup> from the Monte Carlo simulation on the 3D Ising EA model under the  $H$ -shift protocol. The scaling curve is described by

$$Y = X - cX^{1+1/\delta}, \quad (16)$$

for  $X \ll 1$ , where  $c$  is a constant. In Fig. 11(b), for comparison we show the plot of  $Y$  vs  $X$  given by Eq.(16) with  $\delta = 0.81$ , when  $c$  is changed as a parameter. Our data are fitted well with Eq.(16) with  $c = 0.15$  for  $X \leq 0.3$ . Note that when  $c$  and  $\delta$  are adjustable parameters, the least squares fit of the data ( $Y$  vs  $X$ ) ( $0 \leq X \leq 0.6$ ) to Eq.(16) yields the parameters  $c = 0.71 \pm 0.06$  and  $\delta = 0.81 \pm 0.07$ .

In summary, we find a scaling relation that all the set of  $Y = R_{cr}/R_H$  vs  $X = R_W/R_H$  obtained under the  $H$ -shift protocol fall well on a single scaling curve. The curve of  $Y$  vs  $X$  clearly shows a gradual dynamic crossover from the relation  $Y = X$  for  $X \ll 1$  to  $Y \approx 1$  for large  $X$ . In this sense, the  $H$ -shift aging process is nothing but a dynamic crossover from the SG state in  $H = 0$  to the paramagnetic state in  $H > 0$  in the equilibrium limit.

What is the relation between  $H$  and  $T$ , depending on the value of  $X_c$ ? Note that  $X_c \approx 0.1$  for the deviation of  $Y$  from the linear relation  $Y = X$ , and  $X_c \approx 1.6$  for the saturation of  $Y$ . From the relation  $X = X_c$  in Eq.(15a), the magnetic field  $H$  can be derived as

$$H \approx X_c^{1/\delta} \zeta^{1/\delta} (1 - T/T_c)^{a_{eff}} (t_W/\tau_0^*)^{-(b/\delta)T/T_c}. \quad (17)$$

In Fig. 12(a) we show the plot of  $H$  vs  $T$  defined by Eq.(17) as  $X_c$  is varied as a parameter ( $0.5 \leq X_c \leq 1.5$ ), where  $t_W = 1.0 \times 10^4$  sec,  $\tau_0^* = 5.27 \times 10^{-6}$  sec,  $\zeta = 1.5 \times 10^{-4}$ ,  $\delta = 0.81$ ,  $b/\delta = 0.198$ , and  $a_{eff} = 0.55$ . It seems that the  $H$ - $T$  diagram for the fixed  $X_c$  is similar to Eq.(1) with  $p = 3/2$  (the AT prediction). In fact, the least squares fit of these data of  $H$  vs  $T$  to Eq.(1) with  $t_W = 1.0 \times 10^4$  sec for  $2 \leq T \leq 3.6$  K yields the parameters  $A$  and  $p$ . The value of  $p$  is equal to  $1.50 \pm 0.03$ , independent of  $X_c$ , while the value of  $A$  increases as increasing  $X_c$ :  $A = (8.20 \pm 0.15)X_c^{1.31 \pm 0.06}$  [kOe].

Finally we discuss the nature of the line  $T_{g0}(H)$  ( $d\Delta\chi/dT$  vs  $T$ ) shown in Fig. 2. This line is well described by Eq.(1) with  $p = 1.52 \pm 0.10$  and  $A = 3.38 \pm 0.67$  kOe. If the above model is applicable to this line, the value of  $X_c$  is estimated as  $X_c = 0.50$ . Figure 12(b) shows the plot of  $H$  vs  $T$ , where  $H$  is calculated from Eq.(17) for each  $T$ . Here we choose  $t_W = 100$  sec which is appropriate for the measurements of  $\chi_{ZFC}$  and  $\chi_{FC}$ , and  $X_c = 0.28$  which is rather smaller than  $X_c = 0.50$ . We find that the line  $T_{g0}(H)$  ( $d\Delta\chi/dT$  vs  $T$ ) for  $2.5 < T < 3.6$  K lie well on the prediction from Eq.(17). This result also suggests that the line  $T_{g0}(H)$  ( $d\Delta\chi/dT$  vs  $T$ ) is also explained in terms of the droplet picture.

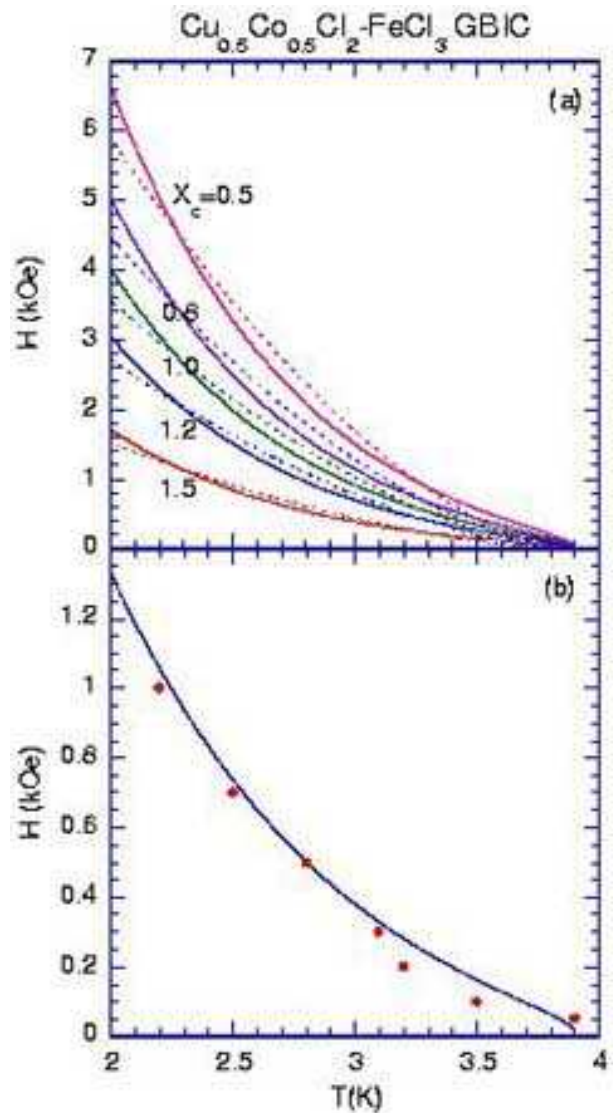


FIG. 12: (Color online) (a)  $H$ - $T$  line (denoted by the solid lines). The value of  $H$  is calculated from Eq.(17) with  $t_W = 1.0 \times 10^4$  sec and  $X_c$  being varied as a parameter ( $0.5 \leq X_c \leq 1.5$ ), where  $\tau_0^* = 5.27 \times 10^{-6}$  sec,  $\zeta = 1.5 \times 10^{-4}$ ,  $\delta = 0.81$ ,  $b/\delta = 0.198$ , and  $a_{eff} = 0.55$ . The dotted lines denote the least-squares fitting curves of the  $H$  vs  $T$  relation for each  $X_c$  to Eq.(1) with  $p \approx 1.5$ . (b)  $H$ - $T$  line. The value of  $H$  as a function of  $T$  is calculated from Eq.(17) with  $X_c = 0.28$  and  $t_W = 100$  sec, where the values of  $\tau_0^*$ ,  $\zeta$ ,  $\delta$ ,  $b/\delta$ , and  $a_{eff}$  are the same as those for (a). The line  $T_{g0}(H)$  ( $d\Delta\chi/dT$  vs  $T$ ) (●) of Fig. 2 is also shown for comparison.

## VI. CONCLUSION

$\text{Cu}_{0.5}\text{Co}_{0.5}\text{Cl}_2\text{-FeCl}_3$  graphite intercalation compound is a three-dimensional short-range Ising SG with a spin freezing temperature  $T_c (= 3.92 \pm 0.11$  K). The stability of the SG phase in the presence of a magnetic field  $H$  has been studied from the spin freezing temperature  $T_f(\omega, H)$  and the peak time  $t_{cr}(T, H)$  of  $S(t)$  vs  $t$  for  $T < T_c$ . We

find that both  $T_f(\omega, H)$  and  $t_{cr}(T, H)$  show certain scaling behavior predicted from the droplet picture. The ratio  $Y (= R_{cr}/R_H)$  is well described by a scaling function of  $X (= R_W/R_H)$  in the form of  $Y = X - cX^{1+1/\delta}$  with  $c = 0.71 \pm 0.06$  and  $\delta = 0.81 \pm 0.07$ . This result indicates the instability of the SG phase in the thermal equilibrium in a finite magnetic field: a dynamic crossover occurs from SG dynamics to paramagnetic behavior.

## Acknowledgments

We would like to thank H. Suematsu for providing us with single crystal kish graphite, and T. Shima and B. Olson for their assistance in sample preparation and x-ray characterization.

- 
- \* itsuko@binghamton.edu  
 † suzuki@binghamton.edu
- <sup>1</sup> See papers in *Spin glasses and random fields*, ed., A.P. Young (World Scientific, Singapore, 1997).
  - <sup>2</sup> M. Mézard, G. Parisi, and M.A. Virasoro, in *Spin Glass Theory and Beyond* (World Scientific, Singapore, 1987) p.59. See also references therein.
  - <sup>3</sup> D.S. Fisher and D.A. Huse, Phys. Rev. Lett. **56**, 1601 (1986); Phys. Rev B **38**, 373 (1988); Phys. Rev. B **38**, 386 (1988).
  - <sup>4</sup> A.J. Bray and M.A. Moore, Phys. Rev. Lett. **58**, 57 (1987).
  - <sup>5</sup> J.R.L. de Almeida and D.J. Thouless, J. Phys. A **11**, 983 (1978).
  - <sup>6</sup> S.F. Edwards and P.W. Anderson, J. Phys. F **5**, 965 (1975).
  - <sup>7</sup> H. Takayama, J. Magn. Magn. Mater. **272-276**, 256 (2004).
  - <sup>8</sup> H. Takayama and K. Hukushima, J. Phys. Soc. Jpn. **73**, 2077 (2004).
  - <sup>9</sup> A.P. Young and H.G. Katzgraber, arXiv: condmat/0407031 (2004).
  - <sup>10</sup> H. Aruga Katori and A. Ito, J. Phys. Soc. Jpn. **63**, 3122 (1994).
  - <sup>11</sup> J. Mattson, T. Jonsson, P. Nordblad, H. Aruga Katori, and A. Ito, Phys. Rev. Lett. **74**, 4305 (1995).
  - <sup>12</sup> P.E. Jönsson, H. Takayama, A. Aruga Katori, and A. Ito, arXiv:cond-mat/0411291 (2004).
  - <sup>13</sup> I.S. Suzuki and M. Suzuki, Phys. Rev. B **68**, 094424 (2003).
  - <sup>14</sup> M. Suzuki and I.S. Suzuki, Eur. Phys. J. B **41**, 457 (2004).
  - <sup>15</sup> L. Lundgren, in *Relaxation in Complex Systems and Related Topics*, edited by I.A. Campbell and C. Giovannella (Plenum Press, New York, 1990) p.3.
  - <sup>16</sup> A.T. Ogielski, Phys. Rev. B **32**, 7384 (1985).
  - <sup>17</sup> G.J.M. Koper and H.J. Hillhorst, J. Phys. France **49**, 429 (1988).
  - <sup>18</sup> R. Hoogerbeets, W.-L. Luo, and R. Orbach, Phys. Rev. B **34**, 1719 (1985).
  - <sup>19</sup> M. Alba, M. Ocio, and J. Hammann, Europhys. Lett. **2**, 45 (1986).
  - <sup>20</sup> M. Suzuki and I.S. Suzuki, submitted to Phys. Rev. B. arXiv:cond-mat/0406473.
  - <sup>21</sup> D. Chu, G.G. Kenning, and R. Orbach, Phil. Mag. B **71**, 479 (1995).
  - <sup>22</sup> N. Bontemps, in *Heidelberg Colloquium on Glassy Dynamics*, edited by J.L. van Hemmen and I. Morgenstern (Springer-Verlag, Berlin, 1986) p.66.
  - <sup>23</sup> N. Bontemps and R. Orbach, Phys. Rev. B **37**, 4708 (1988).
  - <sup>24</sup> P.E. Jönsson, H. Yoshino, and P. Nordblad, Phys. Rev. Lett. **89**, 097201 (2002).
  - <sup>25</sup> P.E. Jönsson, H. Yoshino, and P. Nordblad, Phys. Rev. Lett. **90**, 059702 (2003).